ATMOSPHERIC SCIENCE LETTERS
Atmos. Sci. Let. **17**: 334–338 (2016)
Published online in Wiley Online Library
(wileyonlinelibrary.com) **DOI:** 10.1002/asl.662

RMetS
Royal Meteorological Society

Model study of the asymmetry in tropical cyclone-induced positive and negative surges

Benjamin Wong* and Ralf Toumi

Blackett Laboratory, Space and Atmospheric Physics Group, Imperial College London, UK

**Correspondence to:*
B. Wong, Blackett Laboratory, Space and Atmospheric Physics Group, Imperial College London, Exhibition Road, London SW72AZ, UK.
E-mail: benjamin.wong11@imperial.ac.uk

Received: 15 December 2014
Revised: 24 March 2016
Accepted: 25 March 2016

Abstract

Storm surges pose significant threats to coastal communities, yet negative surges are not as well understood as positive surges. In this study, idealized experiments of a tropical cyclone forcing a 3D ocean model are conducted to investigate the asymmetry of positive and negative surges. Negative surges are larger in magnitude and extend further across the coastline than positive surges. While positive surges are driven by wind blowing onshore, negative surges are largely dominated by alongshore winds, with horizontal divergence as the main mechanism. This asymmetry also increases with decreasing depth and increasing latitude.

Keywords: **negative surge; sea level; asymmetry**

1. Introduction

With 44% of the world's population living within 150 km from the coast (Resio and Westerink, 2008), storm surges are a substantial threat to human lives and activities. Positive surges are widely studied due to the high impacts of coastal flooding but negative surges are less well understood. Some impacts of negative surges include ship grounding and draining of coastal aquifers. Ship grounding can lead to hull damage, subsequent collisions and oil spill disasters. Draining of coastal aquifers can lead to the depletion of drinking water supply and is detrimental to coastal communities dependent on it (Pousa *et al.*, 2013). Negative surges can also destroy coastal aquacultures, which are major economic contributors to countries such as Bangladesh (AsSalek, 1997).

AsSalek (1997) showed that negative surges are affected by factors such as the cyclone's inflow angle, central pressure, radius of maximum winds, speed of translation, propagation path, angle of coastal crossing and interaction with astronomical tides. However, the study was specific to selected points on the unique coastal geometry of the Meghna estuary, making it difficult to apply the same conclusions to other coastal cases. Peng *et al.* (2006) studied positive and negative surges using an idealized coastal setup, investigating the sensitivity of the surges to the cyclone's inflow angle, radius of maximum winds and the speed of translation. However, this idealized study was limited to a one-dimensional (1D) analysis where the positive and negative sea surface height (SSH) response was investigated at a single point. Modelling results of the surge at the Orissa coast of India in 1982 showed a positive surge to the right of the track and a negative surge to the left of the track and this was attributed to winds blowing onshore and offshore respectively (Pugh, 1987). However, the relatively larger negative surges could not simply be accounted for by 1D advection from the onshore and offshore winds. The idealized study performed here provides a basic framework for understanding the asymmetry between the negative and positive surges. We show, for the first time, the importance of the 2D wind field and the important role of the alongshore wind for negative surges.

2. Methods

An idealized tropical cyclone is set up using the wind field as described by Chan and Williams (1987). The domain spans 5° – 35°N and 120° – 180°E at a horizontal resolution of 15 km. The axisymmetric vortex is initialized to the right of the domain at 20°N, 165°E and translated westwards at the speed of 15 km h^{-1} for a total of 8 days. The maximum wind speed is 77 m s^{-1}. The temperature, pressure, humidity, long- and short-wave radiation fields are prescribed to be spatially constant and time-invariant. Increasing the atmospheric pressure has been known to decrease the SSH by 1 cm per mbar (Roden and Rossby, 1999). However, this is a systematic and symmetric change localized near the cyclone centre (runs not shown here). For clarity, the inverse barometer effect, together with other environmental conditions that can affect SSH are not considered here in order to isolate the effect of wind on the asymmetry of storm surges.

The 3D ocean model used is the Regional Ocean Modelling System (ROMS v4.3). ROMS is a free-surface, hydrostatic, primitive equation ocean model that uses stretched, terrain-following coordinates in the vertical and orthogonal curvilinear

© 2016 The Authors. *Atmospheric Science Letters* published by John Wiley & Sons Ltd on behalf of the Royal Meteorological Society.
This is an open access article under the terms of the Creative Commons Attribution License, which permits use, distribution and reproduction in any medium, provided the original work is properly cited.

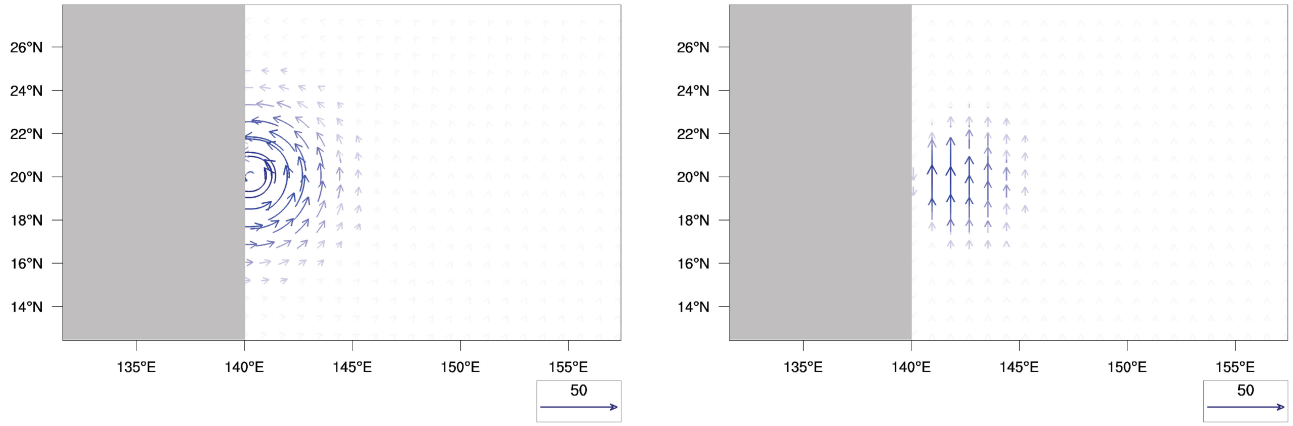


Figure 1. Surface stress (N m^{-2}) response to the total wind stress (a) and to only the alongshore wind stress (b).

coordinates in the horizontal, with Shchepetkin and McWilliams (2005) and Warner *et al.* (2008) outlining the computational algorithms used. The model has 21 vertical levels and a horizontal resolution of 15 km. The initial ocean state has a surface temperature of 28 °C, decreasing linearly to a constant 22 °C from the depth of 500 m and below. The salinity is uniform at 35 psu. The boundaries are closed, with the land mask specified at the western boundary up to 140°E to simulate the coastline.

The 'control' ocean domain has a spatial extent identical to the atmospheric domain (5° – 35°N, 120° – 180°E). The bathymetry is uniform at 100-m deep. The 'higher latitude' case is shifted northwards by 10° (15° – 45°N, 120° – 180°E). The cyclone wind field used to force the ocean model is unchanged, now translating along 30°N instead. The bathymetry is identical to the control setup, uniform at 100 m. A 'sloping bathymetry' case with the same spatial extent as the control case was also studied. The bathymetry slopes linearly eastwards from 50 m near the coast to a maximum of 954 m. The chosen ratio of 1:5000 is an average of the range of coastal slopes studied by Irish *et al.* (2008).

3. Results

Figure 1 shows the surface stress at 105 h when the cyclone crosses the coastline at 140°E. At this time, the alongshore surface stress near the coastline is directed northwards. The cross-shore surface stress (not shown) is westwards to the north of 20°N and eastwards to the south of 20°N. Figure 2 shows the SSH response and the corresponding surface currents at 105 h from initialization. This particular time is chosen to show the maximum magnitude of the positive and negative surges during the event. Not all the cases exhibit their maximum surges at the same time and 105 h was selected for consistency. A later analysis (Figure 3) shows that 105 h is a good representation of the peak surges. The figures are zoomed into 13° – 28°N and 132° – 158°E to display details at the coastline. In the control run (Figure 2(a)), an anticlockwise circulation centering 20°N 142°E is generated with a decrease in SSH at the circulation centre. Along the coastline at 140°E, the magnitude and the alongshore extent of the negative surge are much larger compared to the positive surge (Figure 3). The positive surge is up to +5.3 m and the negative surge is up to −13.1 m. Along the coast, the surface currents flow in the southeastward direction between 18° and 20°N and in the northeastward direction between 13° and 17°N. Figure 2(b) shows the SSH response to only the cross-shore component of the wind stress, with the alongshore component removed. Similar to Figure 2(a), an anticlockwise circulation is generated, but it is elongated zonally and the circulation centre is shifted eastwards to 143°E instead of 142°E. The surge pattern is substantially more symmetrical with a positive surge of up to +4.0 m and a negative surge of only up to −4.5 m.

We next explore the role of the Coriolis parameter in Figure 2(c). A 10° northward shift in latitude shows a greater rightward deflection in the surface currents compared to the control run in Figure 2(a). There is a larger decrease in SSH at the anticlockwise circulation centred at 30°N 142°E. The alongshore extent of the negative surge is much larger compared to the positive surge (Figure 3). The positive surge is decreased from the control case of +5.3 to +4.4 m, but the negative surge is enhanced from the control case of −13.1 to −14.6 m. Without the alongshore wind stress (Figure 2(d)), the positive surge is decreased slightly to +3.9 m but the negative surge is weakened substantially to −5.0 m.

With a sloping bathymetry (Figure 2(e)), there is an overall weaker response in SSH and the ocean currents are less regular. A negative SSH can still be observed at the centre of the anticlockwise circulation. The magnitude and alongshore extent of the negative surge is also much larger compared to the positive surge. The positive surge is up to +4.0 m and the negative surge is up to −6.7 m. In Figure 2(f), the absence of the alongshore wind stress generated a much weaker response in SSH compared to all the other cases. The positive and negative surges are more symmetrical with similar magnitudes of up to 2.8 m.

© 2016 The Authors. *Atmospheric Science Letters* published by John Wiley & Sons Ltd on behalf of the Royal Meteorological Society.

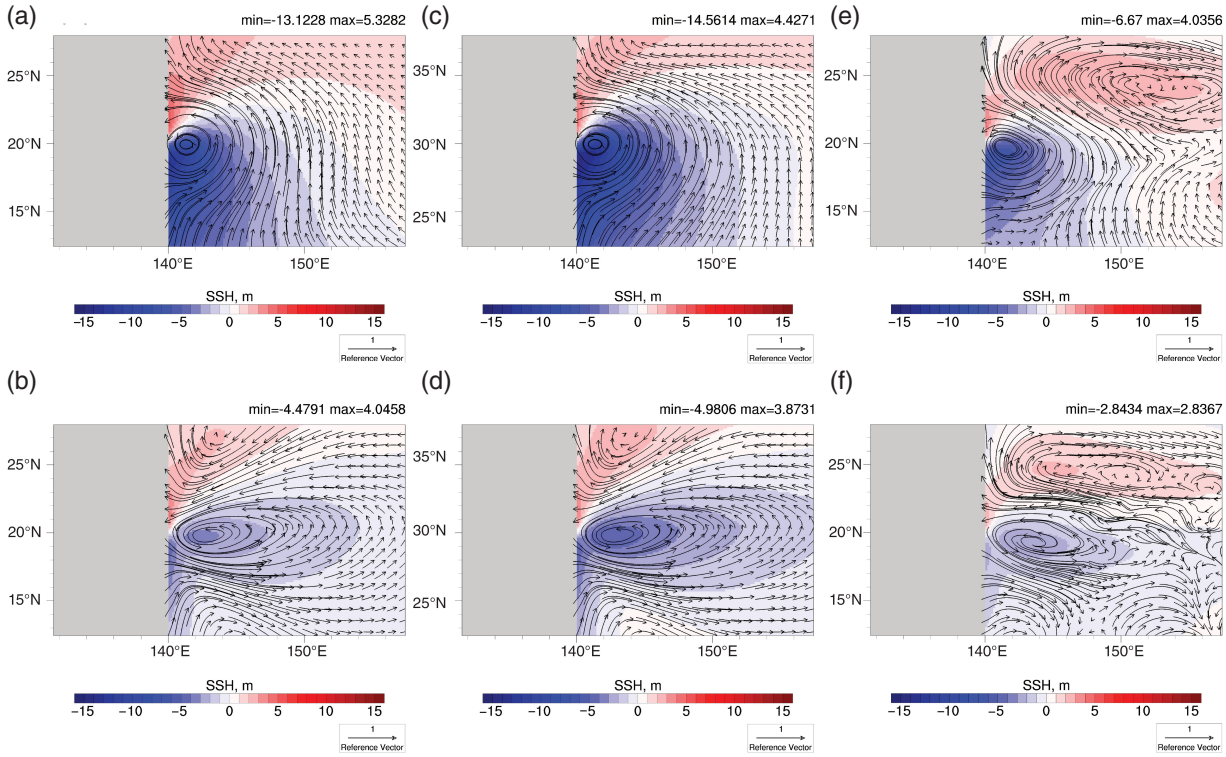


Figure 2. Sea surface height (m) response to the total wind stresses (a, c, e) and to only the cross-shore wind stress (b, d, f): for the control case (a, b), higher latitude case (c, d) and sloping bathymetry case (e, f) at 105 h into the simulation. The reference vector for the sea surface currents is 1 m s^{-1}.

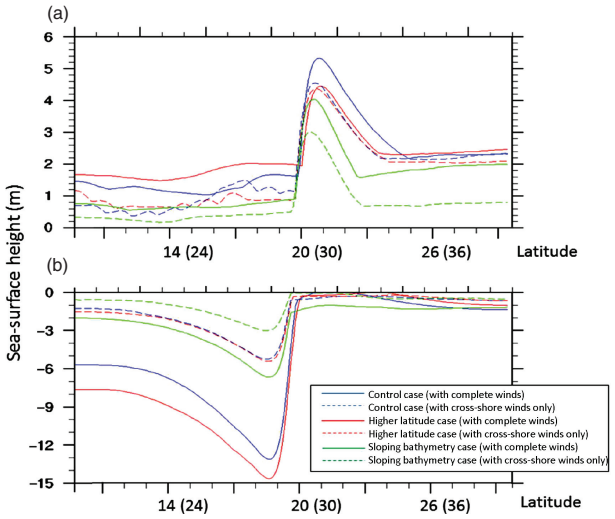


Figure 3. The maximum magnitude of the positive surge (a) and negative surge (b) in meters along the coast line during the simulation for 10 – 30°N (control case) and 20 – 40°N (higher latitude case).

We next examine the peak surges in Figure 3, showing the worst case scenario that the coastline experiences for this event. The three cases with both the cross-shore and alongshore wind stresses show a larger magnitude in the negative surge compared to the positive surge. For the control case, the surge ranges from −13.1 to +5.3 m. The higher latitude case ranges from −14.6 to +4.5 m. The sloping bathymetry case ranges from −6.7 to +4.0 m. The three cases without the alongshore wind stress have comparable positive and negative surges. For the control case, the surge ranges from −5.3 to +4.6 m. The higher latitude case ranges from −5.4 to +4.4 m. The sloping bathymetry case ranges from −3.0 to +3.0 m. These results also confirm the choice of 105 h to map the horizontal extent of the surges for all cases (Figure 2) as the surge at 105 h and the simulation maximum in Figure 3 are very similar.

Figure 3 also shows the horizontal extent that the positive and negative surges affect the coastline. In cases with both the cross-shore and alongshore wind stresses, the positive surge is narrowly distributed along the coast compared to the negative surge which extends far to the south. The cases without the alongshore wind stress show comparably narrow distributions for both the positive and negative surges. As an illustration, the horizontal coastal extent (control case) affected by a positive surge greater than +4 m is 2°, while the region affected by a negative surge larger than −4 m is 20° or more. Without the alongshore wind stress, the coastal region with a positive surge greater than +4 m is halved to about 1°, while the region with a negative surge larger than −4 m is reduced by a factor of 10 to about 2°. Shifting the latitude northwards by 10° reduces the extent of the positive surge to 1° while the extent of the negative surge is increased much further to 25° or more. Without the alongshore wind stress, the region with a positive surge greater than 4 m remains at 1°, while the region with a negative surge larger than −4 m is reduced by a factor of 13 to only 2°. For the sloping bathymetry case, the coastal region impacted by a positive surge

© 2016 The Authors. *Atmospheric Science Letters* published by John Wiley & Sons Ltd on behalf of the Royal Meteorological Society.

greater than 2 m is 2.5°, while the region with a negative surge larger than −2 m is 10°. Without the alongshore wind stress, the region with a positive surge greater than 2 m is reduced to 1.5°, while the region impacted by a negative surge larger than −2 m is only 2.5°.

4. Discussion

A mechanism has been proposed by Peng *et al.* (2006) to account for the 1D asymmetry in the sea level response, where the pressure gradient force required to balance the wind is a function of $(h+\zeta)\mathrm{d}\zeta/\mathrm{d}x$ (where h, ζ, x are the undisturbed water depth, the sea surface elevation and distance from the coast, respectively). This 1D analysis explains the basic asymmetry in positive and negative surges, since it is easier to move the lower water mass for a negative surge, given the same wind. However, observations and analyses described by Pugh (1987) and Pousa *et al.* (2013) showed horizontal surge features that a 1D mechanism cannot fully represent quantitatively.

The idealized study here provides a basic spatial framework for the understanding of cyclone-driven surges and the asymmetry between positive and negative surges. In the absence of the alongshore wind stress (Figure 2(b)), the coastal surge pattern is more symmetrical along 20°N. The anticlockwise circulation is elongated along 20°N since only the cross-shore wind stress is present. The centre of the anticlockwise circulation is shifted eastwards with the western land-mask acting as a barrier, shifting the elongated water mass eastwards. The northward alongshore wind stress generates a northward advection of water mass that increases the positive surge and decreases the negative surge. In addition, Ekman transfer of momentum deflects the northward alongshore flow rightwards, decreasing the overall SSH at the coast. Without the alongshore wind stress, the two effects oppose in the case of the positive surge, showing an overall decrease from +5.3 to +4.0 m. For the negative surge, the two effects add up and resulted in a substantial decrease in the magnitude of the negative surge from −13.1 to −4.5 m. This substantial additional decrease demonstrates that the alongshore component of the wind stress plays a very important role in creating the horizontal divergence that is the main driver of the negative surge. Surges simply generated by onshore and offshore winds alone generate fairly symmetrical surge patterns as shown in Figure 2(b). In the case of a southern hemisphere scenario, the tropical cyclone will be rotating clockwise, creating a southward alongshore component in the same domain setup. The results will be inverted but conceptually the same.

When the ocean domain is shifted northwards by 10° (comparing Figures 2(a) and 2(c)), the ocean currents are deflected more towards the right with the enhanced Coriolis force. The increased rightward deflection of the northward alongshore surface stress decreases both the positive and negative surges. Comparing Figures 2(b) and 2(d), both the positive and negative surges decrease in magnitude with the weakened cross-shore stress that resulted from the enhanced rightward deflection. The enhanced rightward deflection also increases the outward divergence of the anticlockwise circulation, resulting in a greater decrease in the SSH here. Overall, both the positive and negative surge decreases. That the Coriolis force affects the extent of negative storm surge is not a surprise since the storm negative surges are driven by horizontal divergence. This cannot be accounted for by 1D mechanisms.

While the previous two cases represent a near-shore or continental shelf scenario, the sloping bathymetry case (Figures 2(e) and 2(f)) shows a different scenario where the cyclone approaches the coastline from deep waters. As the response of the SSH to wind stress is inversely proportional to the depth of the water column (Pugh, 1987), the deeper water shows a weaker SSH response compared to the shallower cases. While the sloping bathymetry case produced smaller magnitude and range in asymmetry between the positive and negative surges, it delivers the same qualitative message as the control case. The asymmetry in the magnitude and horizontal extent of the positive and negative surges is still substantial, with horizontal divergence as the main driver of this asymmetry. The absence of the alongshore wind stress component generates a fairly symmetrical surge response that is expected from having onshore and offshore winds alone.

The surge asymmetry can be characterized by the ratio defined as $\frac{\zeta^-}{\zeta^+}$ (where ζ^- and ζ^+ are the magnitudes of the minimum and the maximum SSH at the coast, respectively). In the control case, the alongshore wind stress increases the ratio from 1.2 to 2.5, demonstrating the significance of the alongshore wind stress in generating the large asymmetry. With a 10° northward shift in latitude, the asymmetry increases to 3.2. This increase is expected with horizontal divergence as the main mechanism for driving the negative surges. A deeper and sloping bathymetry lowers the ratio to 1.7, illustrating the effect of the deeper waters weakening the SSH response. The surge ratios for the storms at the Orissa coast in 1982 (Pugh, 1987) and the Argentinian coast in 1984 (Pousa *et al.*, 2013) are 2.7 and 1.9, respectively, both of which are well within the range estimated in this study.

The asymmetry in the horizontal extent of the positive and negative surges along the coastline has not been noted in literature. Comparing the horizontal extent of the positive and negative surges in Figure 3 shows that the alongshore wind stress is the main contributor to this large asymmetry. In the control case, the negative surge affected coastal regions by a factor of 10 compared to the positive surge. Without the alongshore wind stress, the asymmetry decreases by a factor of 2. Increasing the latitude by 10° northwards raises this asymmetry to 25 but in the absence of the alongshore component, the asymmetry decreases to 2. For the sloping bathymetry case, the extent of the negative surge is four times larger than the positive surge. Without the alongshore wind stress, the coastal extent affected by

© 2016 The Authors. *Atmospheric Science Letters* published by John Wiley & Sons Ltd on behalf of the Royal Meteorological Society.

the negative surge is only a factor of 1.7 larger than the positive surge. This comparison in horizontal extents gave a similar conclusion as the surge ratios discussed previously. The simulation results of Pugh (1987) for the storm hitting the Orissa coast of India also show the negative surge affecting a greater coastal extent than the positive surge.

5. Conclusion

Storm surges can result in high economic consequences and even the loss of lives. While the impacts and occurrences of positive surges are widely investigated, negative surges are less understood. Existing studies on negative surges have been limited to either specific real case studies with specific inferences, or idealized studies that do not consider the horizontal extent of the SSH response. In this study, the asymmetry of positive and negative surges in the magnitude and spatial extent is investigated using idealized experiments. Three cases have been examined. While the occurrence of positive and negative surges has previously been understood as being driven by winds blowing onshore and offshore, respectively, the wind stress experiments here reveal that the alongshore component is the main cause of asymmetry in the magnitude and spatial scale of the surge. We further examine the sensitivity of the asymmetry to latitude and bathymetry. The asymmetry increases with increasing Coriolis force. A northward shift in latitude increases the asymmetry. The third case investigates the SSH response in a deeper, sloping ocean floor. The overall SSH response for this case is weaker than the shallower cases and the surge asymmetry decreases. The alongshore wind stress is also the main contributor to the large asymmetry in the length of coastline affected by the positive and negative surges. This study shows that positive and negative surges have some similarities but also different causes and properties. Simplified storm surge models that only incorporate cross-shore winds to analyse the positive and negative surges will not capture the large asymmetry shown here.

References

AsSalek JA. 1997. Negative surges in the Meghna estuary in Bangladesh. *Monthly Weather Review* **125**(7): 1638–1648, doi: 10.1175/1520-0493(1997)125<1638:Nsitme>2.0.Co;2.

Chan JCL, Williams RT. 1987. Analytical and Numerical-Studies of the Beta-Effect in Tropical Cyclone Motion. Part 1: zero mean flow. *Journal of the Atmospheric Sciences* **44**(9): 1257–1265, doi: 10.1175/1520-0469(1987)044<1257:Aansot>2.0.Co;2.

Irish JL, Resio DT, Ratcliff JJ. 2008. The influence of storm size on hurricane surge. *Journal of Physical Oceanography* **38**(9): 2003–2013, doi: 10.1175/2008jpo3727.1.

Peng MC, Xie L, Pietrafesa LJ. 2006. Tropical cyclone induced asymmetry of sea level surge and fall and its presentation in a storm surge model with parametric wind fields. *Ocean Model* **14**(1–2): 81–101, doi: 10.1016/j.ocemod.2006.03.004.

Pousa JL, D'Onofrio EE, Fiore MME, Kruse EE. 2013. Environmental impacts and simultaneity of positive and negative storm surges on the coast of the Province of Buenos Aires, Argentina. *Environmental Earth Sciences* **68**(8): 2325–2335, doi: 10.1007/s12665-012-1911-9.

Pugh DT. 1987. *Tides, Surges and Mean Sea-Level*. John Wiley and Sons: Chichester, UK.

Resio DT, Westerink JJ. 2008. Modeling the physics of storm surges. *Physics Today* **61**(9): 33–38, doi: 10.1063/1.2982120.

Roden GI, Rossby HT. 1999. Early Swedish contribution to oceanography: Nils Gissler (1715–71) and the inverted barometer effect. *Bulletin of the American Meteorological Society* **80**(4): 675–682, doi: 10.1175/1520-0477(1999)080<0675:Escton>2.0.Co;2.

Shchepetkin AF, McWilliams JC. 2005. The regional oceanic modeling system (ROMS): a split-explicit, free-surface, topography-following-coordinate oceanic model. *Ocean Model* **9**(4): 347–404, doi: 10.1016/j.ocemod.2004.08.002.

Warner JC, Sherwood CR, Signell RP, Harris CK, Arango HG. 2008. Development of a three-dimensional, regional, coupled wave, current, and sediment-transport model. *Computers & Geosciences* **34**(10): 1284–1306, doi: 10.1016/j.cageo.2008.02.012.

© 2016 The Authors. *Atmospheric Science Letters* published by John Wiley & Sons Ltd on behalf of the Royal Meteorological Society.